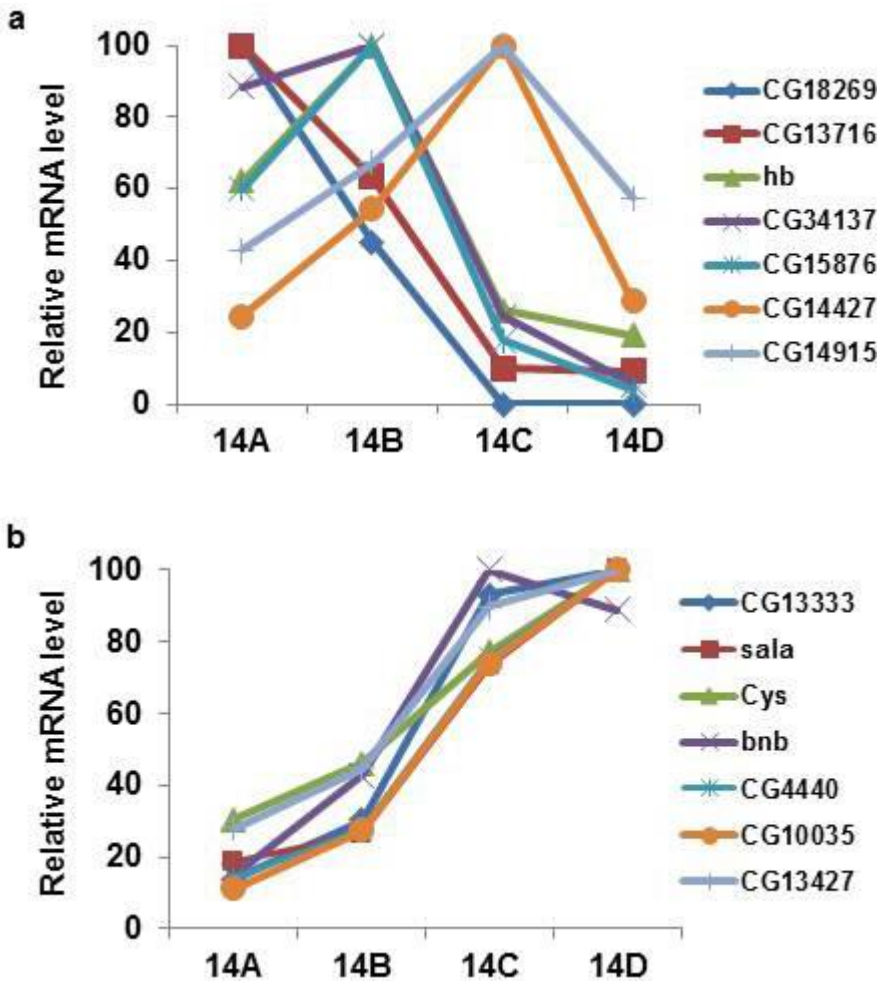

Supplementary Fig. S1. mRNA profiles during MBT. (**A**) Shown are expression levels of representative genes that exhibit properties of transcription shutdown during nc14 (see Supplementary Table S1 for a complete list). CG18269 and CG13716 exhibit a shutdown starting at stage 14A, *hb*, CG34137 and CG 15876 at 14B, and CG14427 and CG14915 at 14C. (**B**) Shown are expression levels of representative early-expressing genes without exhibiting properties of shutdown at nc14. The seven genes shown were chosen from the non-shutdown gene category with the highest RPKM (see Materials and Methods). In both panels mRNA levels for each gene were normalized with its peak level (set as 100).

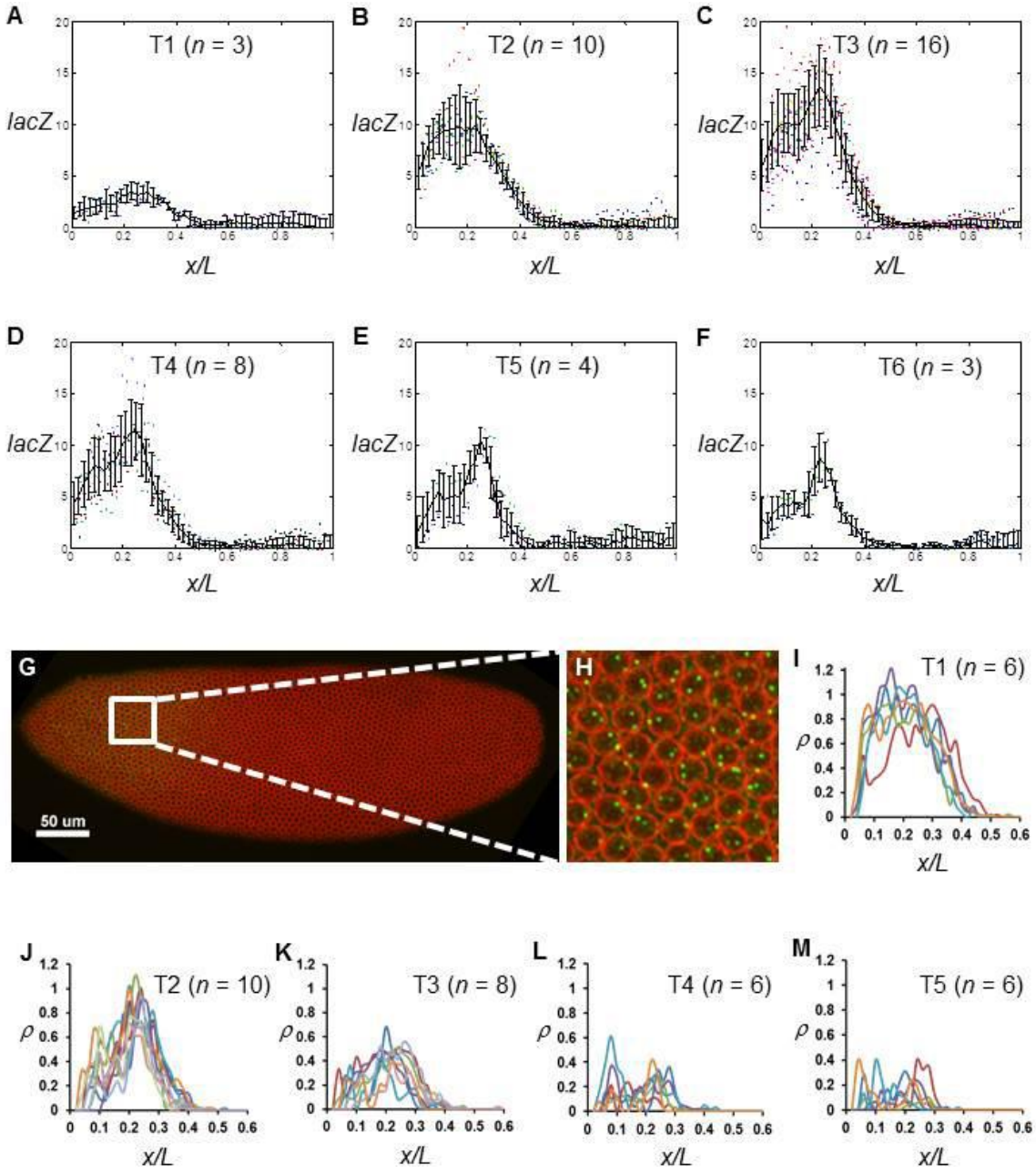

Supplementary Fig. S2. Temporal dynamics of *bcd6-lacZ* reporter gene transcription. (**A-F**) Intensity profiles of *lacZ* mRNA (in arbitrary units, a.u.) extracted from individual embryos at the indicated time classes. The mean and standard deviation (s.d.) are also shown. (**G,H**) An image showing the nascent *lacZ* transcripts detected as discrete fluorescent dots and the nuclear envelope shown in red. (**I-M**) ρ profiles of *bcd6-lacZ* transcription extracted from individual embryos at the indicated time classes. Each profile represents data from one embryo and is shown by one color in a panel.

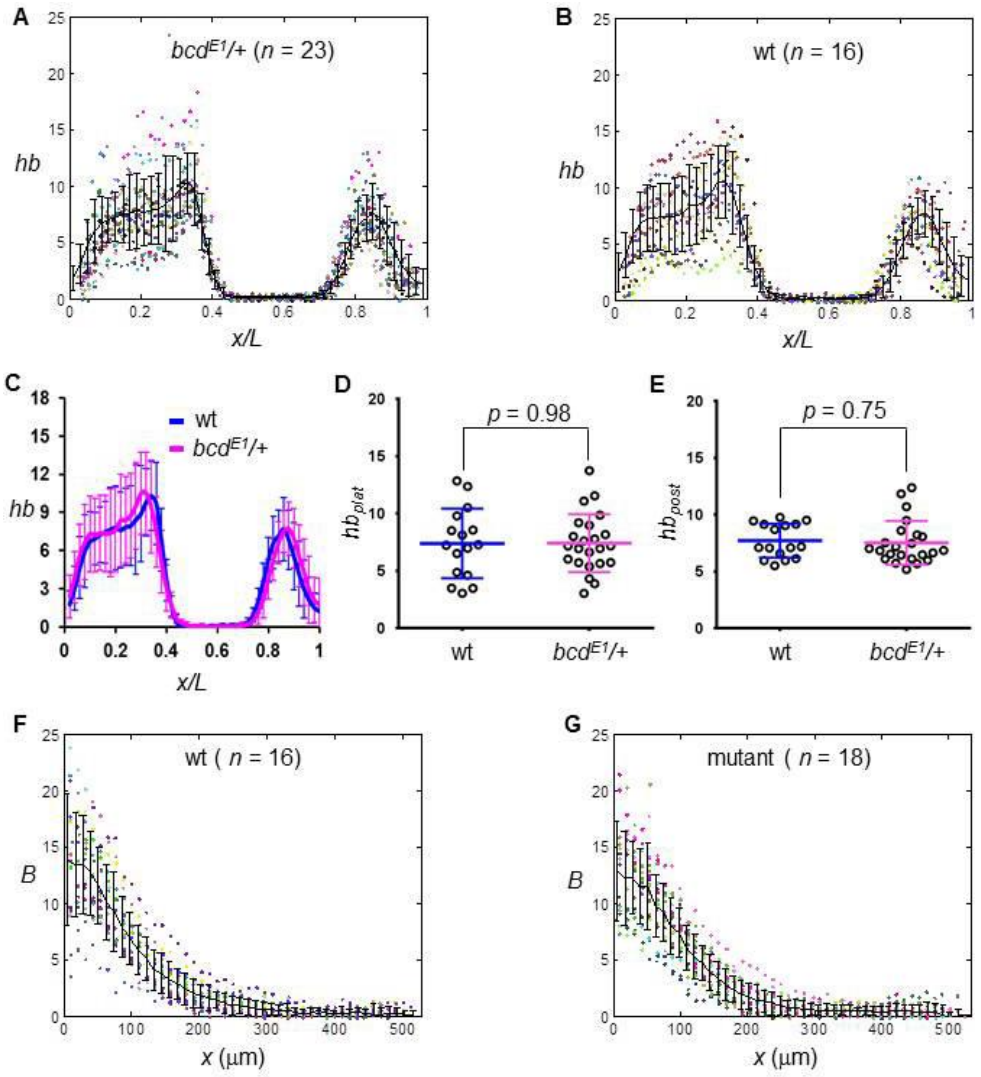

Supplementary Fig. S3. *hb* and Bcd properties are insensitive to maternal *bcd* gene source (endogenous or transgenic). (**A,B**) Intensity profiles of *hb* mRNA (in a.u.) extracted from individual embryos derived from mothers with a copy of either the endogenous wt *bcd* gene or a wt *bcd* transgene (referred to as the bcd^{E1}/+ and "wt" embryos—see main text). (**C**) The mean *hb* intensity profile from bcd^{E1}/+ and wt embryos. (**D,E**) Shown are hb_{plat} and hb_{post} values from individual wt and bcd^{E1}/+ embryos. The mean hb_{plat} and s.d. are 7.42 ± 2.53 and 7.39 ± 3.03 and the mean hb_{post} and s.d. are 7.53 ± 1.93 and 7.71 ± 1.50 in wt and bcd^{E1}/+ embryos, respectively. (**F,G**) Shown are Bcd intensity profiles (in a.u.) from individual wt and mutant embryos derived from transgenic flies (see Fig. 3a for a plot showing the super-imposed mean profiles).

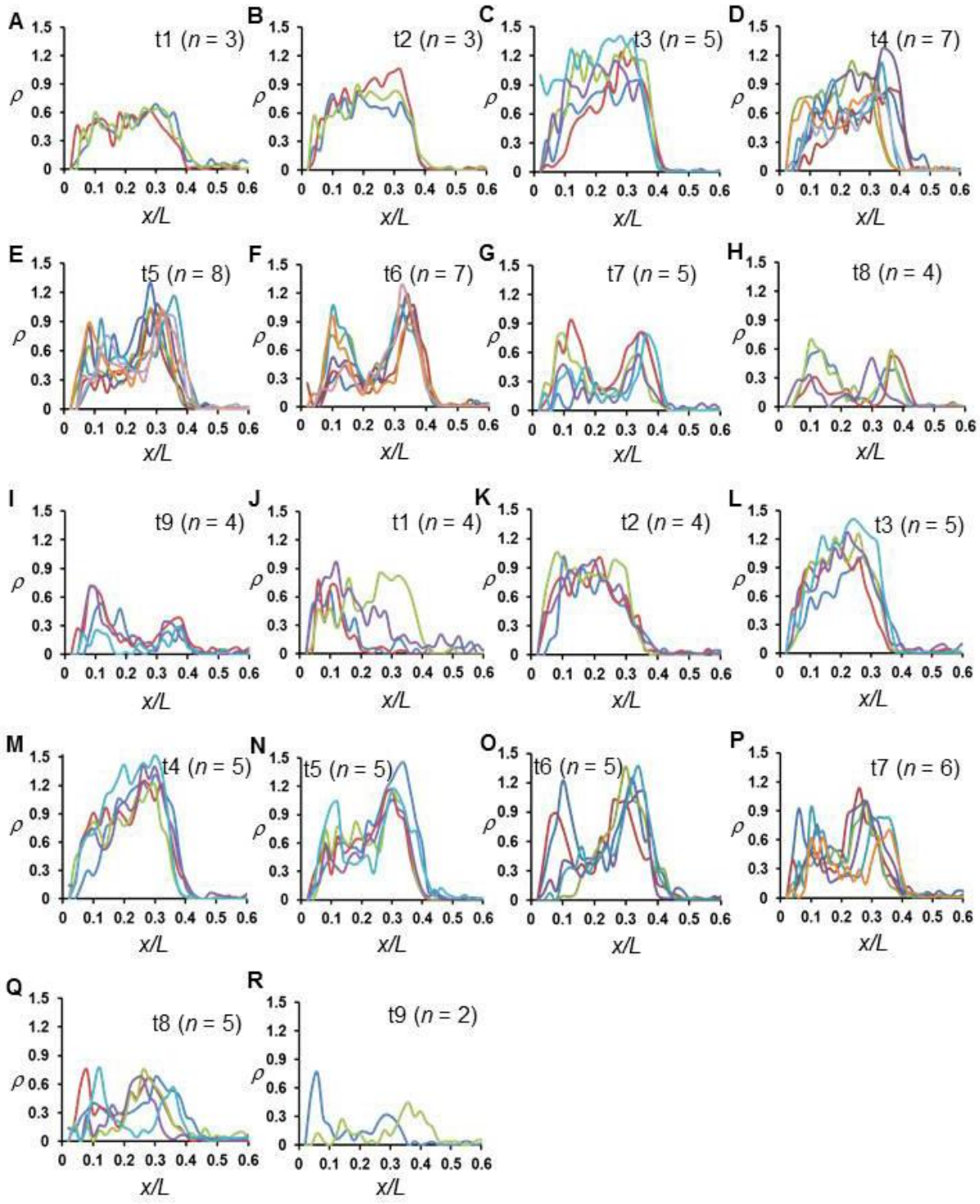

Supplementary Fig. S4. ρ profiles of active *hb* transcription as a function of AP position *x*/*L*. Data are extracted from individual wt (**A-I**) and mutant (**J-R**) embryos at the indicated time classes. Each color in a panel represents data from one embryo.

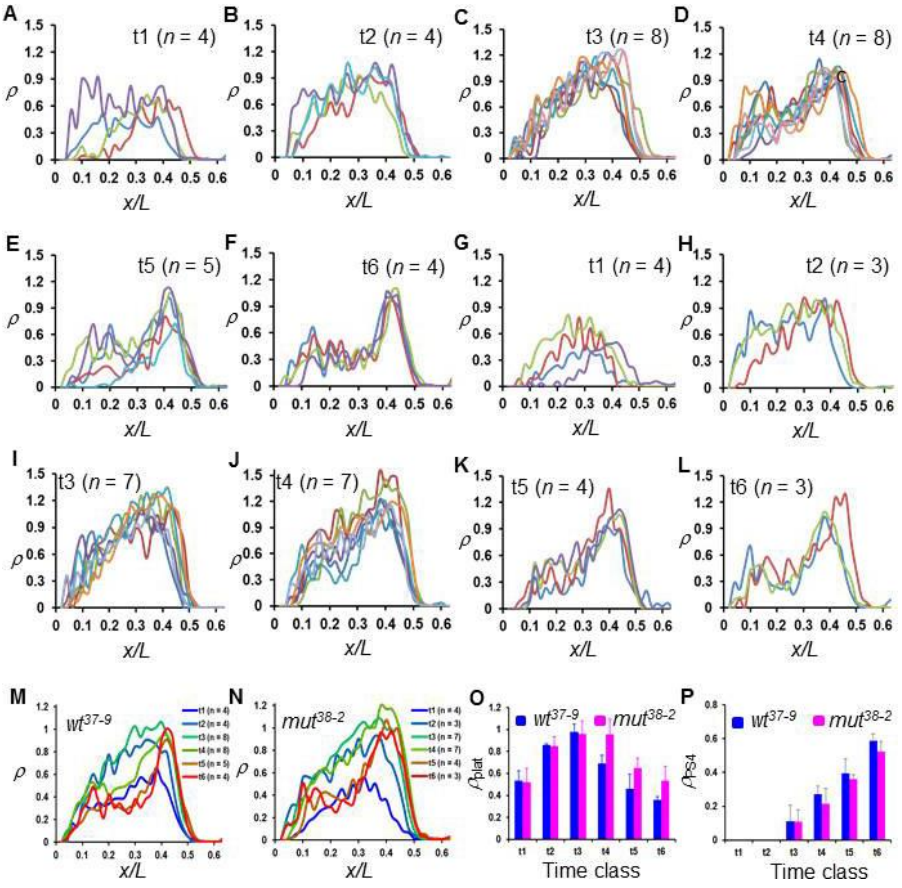

Supplementary Fig. S5. Postponement in *hb* shutdown detected in embryos derived from an alternate pair of wt and mutant *bcd* transgenic lines. (**A-L**) ρ profiles of *hb* extracted from individual embryos derived from mothers containing two copies of wt (**A-F**) or mutant (**G-L**) *bcd* gene generated from standard P-element mediated transformation (referred to as the $wt^{37\text{-}9}$ and $mut^{38\text{-}2}$ embryos, respectively) at the indicated time classes. (**M,N**) Shown are mean ρ profiles of *hb* in $wt^{37\text{-}9}$ and $mut^{38\text{-}2}$ embryos at the indicated time classes. (**O,P**) Shown are the mean and s.d. of ρ_{plat} and ρ_{PS4} in $wt^{37\text{-}9}$ and $mut^{38\text{-}2}$ embryos at different time classes. The *p* values for ρ_{plat} between wt and mutant embryos are: 0.87, 0.83, 0.71, 4.0×10^{-4}, 4.6×10^{-2} and 4.8×10^{-2} for t1 to t6, respectively. The ρ_{PS4} values at t1 and t2 are not available in panel **P** because active transcription specific to PS4 is not yet detectable at these times. The *p* values for ρ_{PS4} between wt and mutant embryos are: 0.96, 0.14, 0.46 and 0.16 for t3 to t6, respectively.

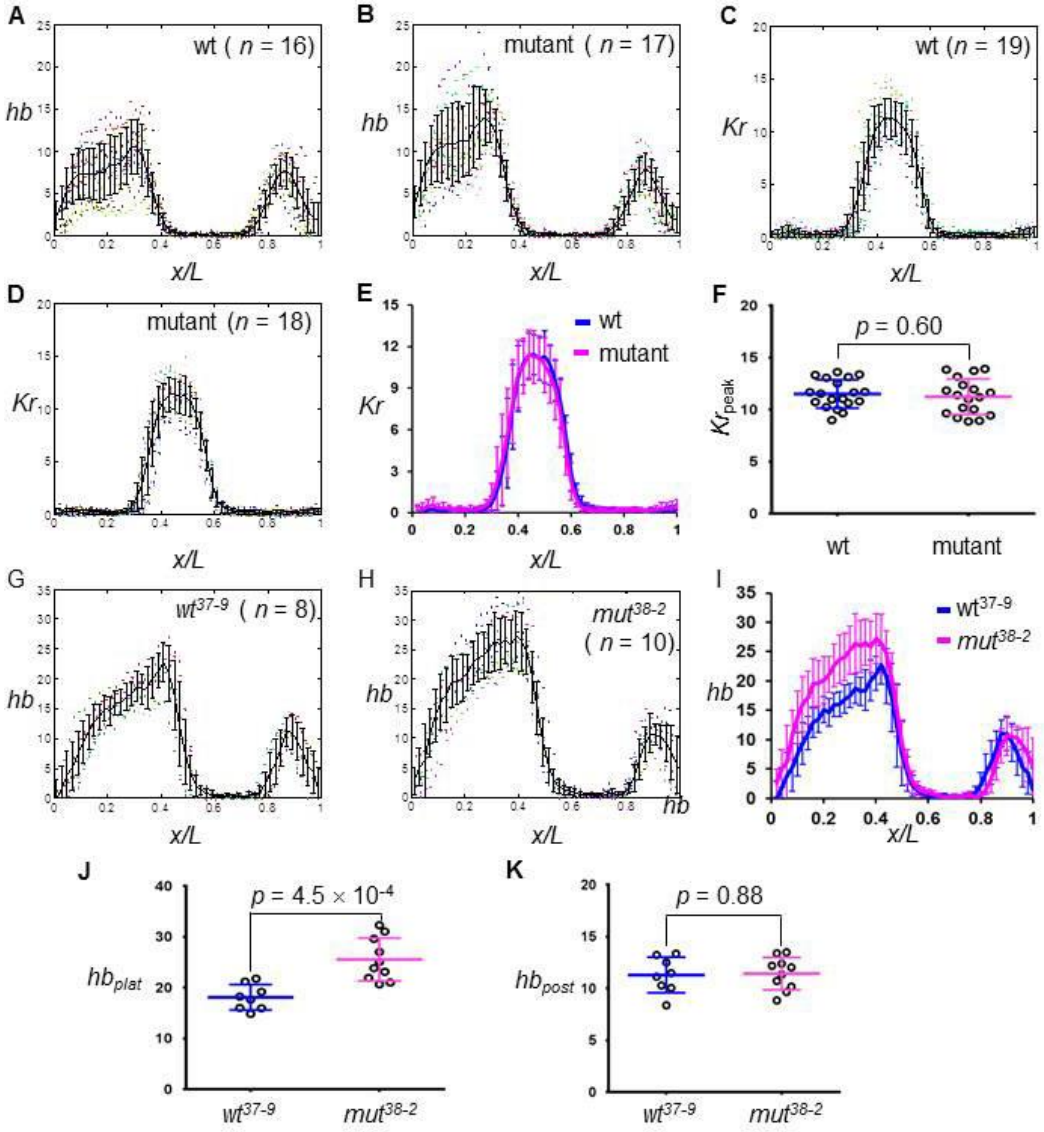

Supplementary Fig. S6. *hb* mRNA level is increased by Bcd sumoylation mutation. (**A,B**) Intensity profiles of *hb* mRNA (in a.u.) extracted from individual wt and mutant embryos, with mean and s.d. given. (**C,D**) Intensity profiles of *Kr* mRNA (in a.u.) extracted from individual wt and mutant embryos. (**E**) The mean intensity profile of *Kr* mRNA from wt and mutant embryos. (**F**) Shown are individual Kr_{peak} values from wt and mutant embryos. The mean Kr_{peak} and s.d. are 11.51 ± 1.36 and 11.24 ± 1.71 in wt and mutant embryos, respectively. (**G,H**) Intensity profiles of *hb* mRNA extracted from individual $wt^{37\text{-}9}$

and *mut*$^{38\text{-}2}$ embryos. (**I**) The mean intensity profile of *hb* mRNA from *wt*$^{37\text{-}9}$ and *mut*$^{38\text{-}2}$ embryos. (**J,K**) Shown are the individual hb_{plat} and hb_{pos} values from *wt*$^{37\text{-}9}$ and *mut*$^{38\text{-}2}$ embryos. The mean hb_{plat} is increased from 18.11 ± 2.51 in wt to 25.57 ± 4.23 in mutant embryos ($p = 4.5 \times 10^{-4}$) while the mean hb_{post} is unaffected: 11.30 ± 1.71 and 11.42 ± 1.56 in wt and mutant embryo, respectively ($p = 0.88$).

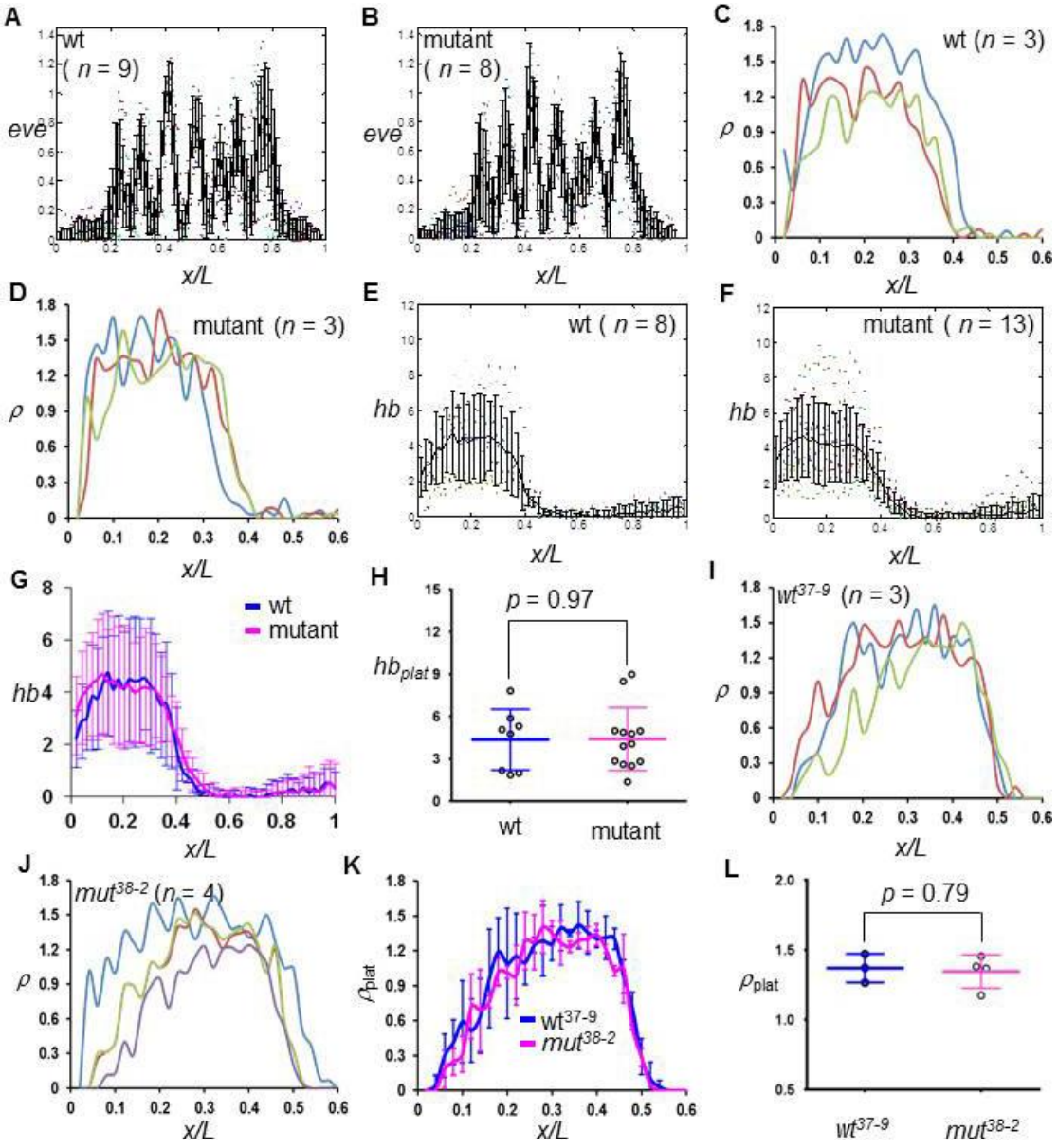

Supplementary Fig. S7. Individual *eve* intensity profiles at nc14 and *hb* transcription profiles at nc13. (**A,B**) Normalized intensity profiles of *eve* mRNA extracted from individual wt and mutant embryos at nc14. (**C,D**) ρ profiles of *hb* transcription in individual wt and mutant embryos at nc13. (**E,F**) Intensity profiles of *hb* mRNA extracted from individual wt and mutant embryos. (**G**) The mean intensity profiles of *hb* mRNA from wt and mutant embryos at nc13. (**H**) Shown are hb_{plat} levels (in a.u.) of individual wt and mutant

embryos at nc13. The mean hb_{plat} and s.d. are 4.35 ± 2.16 and 4.39 ± 2.24 in wt and mutant embryos (p = 0.97). (**I,J**) ρ profiles of *hb* extracted from individual $wt^{37\text{-}9}$ and $mut^{38\text{-}2}$ embryos at nc13. (**K**) ρ profiles of *hb* from $wt^{37\text{-}9}$ and $mut^{38\text{-}2}$ embryos at nc13. (**L**) Shown are ρ_{plat} values measured in individual $wt^{37\text{-}9}$ and $mut^{38\text{-}2}$ embryos at nc13. The mean ρ_{plat} and s.d. are 1.37 ± 0.10 and 1.35 ± 0.12 in wt and mutant embryos (p = 0.79).

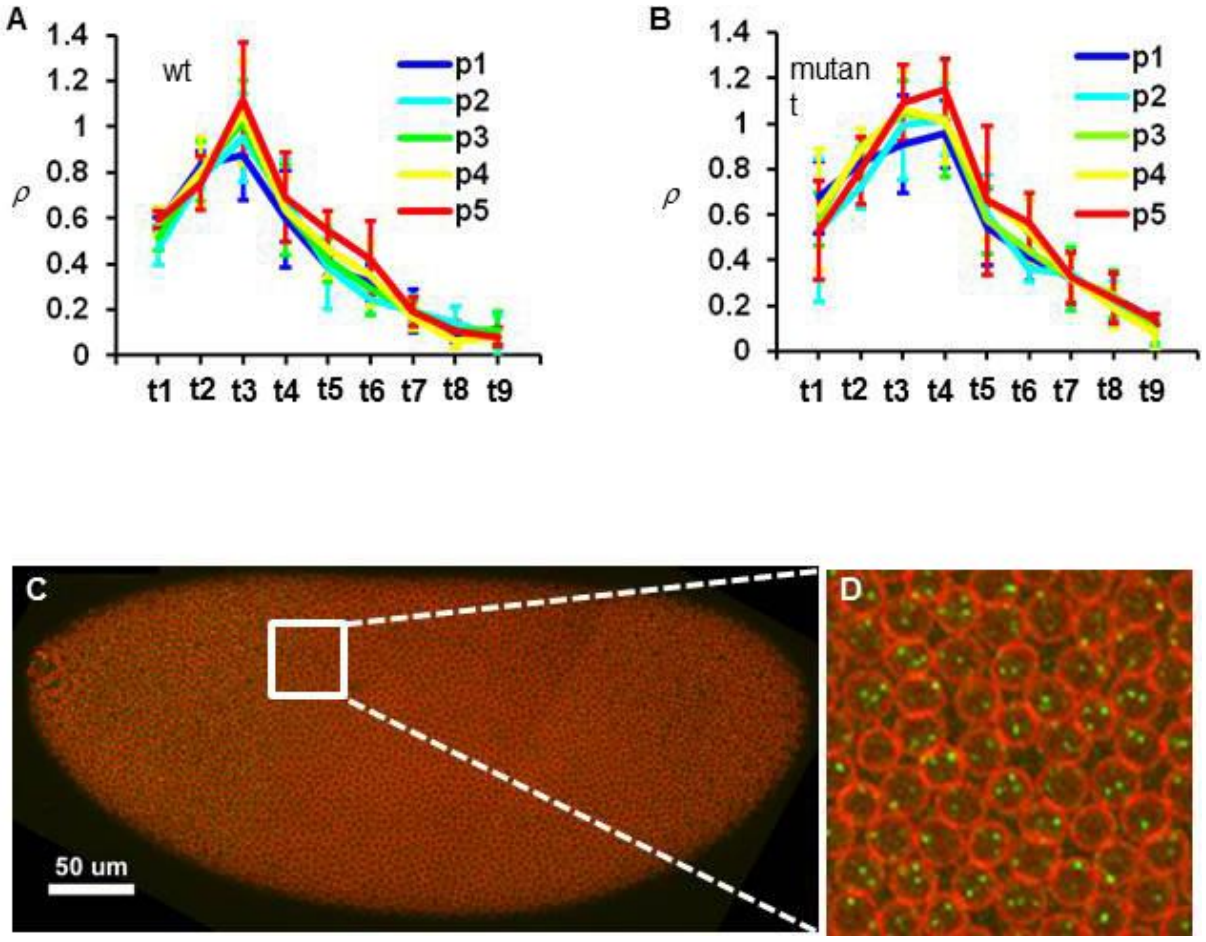

Supplementary Fig. S8. *hb* transcription shutdown is neither position-dependent nor triggered by DNA replication. (**A,B**) ρ profiles as a function of time class t from the five individual bins at the plateau region of wt and mutant embryos; here p1 represents the most anterior bin in the plateau, while p5 the most posterior. For either wt or mutant embryos, there is no indication of time-dependent "spreading" of shutdown from posterior to anterior in the plateau region. (**C,D**) An image of a wt embryo with intron dots shown in green and nuclear envelope in red. Note that many nuclei have >2 bright intron dots detected, indicating that DNA replication has taken place at the *hb* locus in these nuclei.

Supplementary Table S1 List of shutdown genes (total of 194)

ac	CG10877	CG14787	CG32711	CG6885	Cyp312a1	hbn	N	RpLP2	Tfb5
Ac78C	CG10880	CG14915	CG3363	CG7197	dod	hkb	NetA	RpS5b	tld
Act5C	CG11092	CG15382	CG34137	CG7271	dpp	hop	Neu2	RpS6	tll
alt	CG11190	CG15634	CG34214	CG7288	dsh	hrg	Nmt	run	Tom40
Amun	CG11444	CG15876	CG34266	CG7326	Dsp1	I-2	numb	S6kII	tsg
Apc2	CG11534	CG16890	CG34401	CG7332	east	kni	oc	sc	wal
Ate1	CG11582	CG17829	CG34422	CG7598	Egfr	l(1)G0334	os	scw	wech
bmm	CG11943	CG18269	CG3446	CG7872	egh	l(1)sc	Pep	shn	wee
bnk	CG12424	CG1908	CG3527	CG8184	Eip71CD	l(2)08717	Pepck	sick	wntD
brk	CG13000	CG1968	CG3638	CG8369	ERR	Lnk	ph-p	snRNP-U1-70K	yu
Bro	CG13366	CG2158	CG42516	CG8924	esg	m4	Pink1	sog	z
Bsg25A	CG13653	CG2247	CG42553	CG8928	exba	Mad	Pkn	Spt6	Z600
Bsg25D	CG13711	CG2469	CG42558	CG9281	exd	MAN1	Pp2C1	Spx	ZC3H3
Bub1	CG13713	CG2712	CG42575	CG9425	Exp6	Mgat2	PpV	SRm160	zen
bun	CG13716	CG2918	CG4570	CG9773	fend	mip130	Psf3	Sry-alpha	
Bx42	CG14014	CG3033	CG4575	CG9915	fliI	Mis12	Ptp4E	stwl	
Cct1	CG14050	CG30431	CG4702	Corp	gk	mnd	Rab40	Su(var)2-HP2	
Cdk7	CG14317	CG3149	CG4785	Cpr60D	gt	mRpL14	Rab8	Sur-8	
CG10347	CG14427	CG3226	CG5830	crn	halo	mRpL3	retn	Taf4	
CG10555	CG14476	CG3238	CG6455	cv	hb	mud	rib	tay	

Supplementary Table S2 Functional enrichment of shutdown genes

Category	Term	No. of genes	P-value (Bonferroni)
SP_PIR_KEYWORDS	developmental protein	35	2.14E-11
GOTERM_BP_FAT	GO:0048598~embryonic morphogenesis	23	4.40E-09
GOTERM_BP_FAT	GO:0045165~cell fate commitment	23	7.46E-09
GOTERM_BP_FAT	GO:0007354~zygotic determination of anterior/posterior axis, embryo	11	1.07E-08
INTERPRO	IPR007970:Protein of unknown function DUF733	7	2.87E-07
GOTERM_BP_FAT	GO:0003002~regionalization	28	1.21E-06
GOTERM_BP_FAT	GO:0001703~gastrulation with mouth forming first	10	3.11E-06
GOTERM_BP_FAT	GO:0010004~gastrulation involving germ band extension	10	3.11E-06
GOTERM_MF_FAT	GO:0030528~transcription regulator activity	34	6.16E-07
GOTERM_MF_FAT	GO:0016566~specific transcriptional repressor activity	10	6.44E-07
GOTERM_BP_FAT	GO:0007389~pattern specification process	28	4.13E-06
GOTERM_MF_FAT	GO:0003677~DNA binding	37	1.83E-06
GOTERM_BP_FAT	GO:0007369~gastrulation	12	1.33E-05
GOTERM_BP_FAT	GO:0007167~enzyme linked receptor protein signaling pathway	15	5.45E-05
GOTERM_BP_FAT	GO:0009952~anterior/posterior pattern formation	16	5.91E-05
GOTERM_BP_FAT	GO:0001709~cell fate determination	14	1.02E-04
GOTERM_MF_FAT	GO:0016564~transcription repressor activity	13	2.60E-05
GOTERM_BP_FAT	GO:0048732~gland development	15	2.38E-04
GOTERM_BP_FAT	GO:0006357~regulation of transcription from RNA polymerase II promoter	16	2.96E-04
GOTERM_BP_FAT	GO:0007419~ventral cord development	8	4.21E-04
GOTERM_BP_FAT	GO:0051252~regulation of RNA metabolic process	30	4.33E-04
GOTERM_BP_FAT	GO:0009880~embryonic pattern specification	17	5.97E-04
GOTERM_BP_FAT	GO:0006355~regulation of transcription, DNA-dependent	28	6.53E-04